CMMoST 2019

5th INTERNATIONAL CONFERENCE ON

Mechanical Models in Structural Engineering

Alicante, SPAIN
23 - 25 October 2019
Escuela Politécnica Superior
Universidad de Alicante

Full Papers

Universitat d'Alacant
Universidad de Alicante

UNIVERSIDAD DE GRANADA

CMMoST 2019

5th INTERNATIONAL CONFERENCE ON

Mechanical Models in Structural Engineering

Polytechnic School of Alicante

23rd – 25th October 2019

Universitat d'Alacant
Universidad de Alicante

ugr

UNIVERSIDAD D SEVILLA

Edita: Editorial Club Universitario
C/ Decano, n.º 4 – 03690 San Vicente (Alicante)
www.ecu.fm
original@ecu.fm

ISBN: 978–84–17924–58–4
ISBN papel: 978–84–17924–22–5

Printed in Spain

Organizan:

Universitat d'Alacant
Universidad de Alicante

ugr

UNIVERSIDAD D SEVILLA

Patrocinan:

MAPEI®
ADHESIVES·SEALANTS·CHEMICAL PRODUCTS FOR BUILDING

PAVASAL

CONTENTS

5th International Conference on Mechanical Models in Structural Engineering
CMMoST 2019
23-25 oct 2019 Alicante SPAIN

Motion-based design of viscous dampers for cable-stayed bridges under uncertainty conditions

Naranjo-Pérez, Javier[1]; Jiménez-Alonso, Javier Fernando[2]; Díaz, Iván M.[3]; Sáez, Andrés[4]

ABSTRACT

Passive damping devices are widely installed to control the vibration level of stay cables of bridges induced by wind action. The design of passive damping devices must ensure the performance for the all the life-cycle of the structure. In this sense, the design should consider the changes of the pre-fixed parameters and environmental conditions. For this purpose, the motion-based design method under uncertainty conditions is used in this study to carry out the design of a viscous damper. Following this approach, the design requirements are established according to the maximum accepted motions of the structure and the damper device is optimized. In order to validate the method, a benchmark structure is considered. The uncertainty conditions are numerically simulated following a probabilistic approach. As simulation method, the Latin Hypercube is employed. The reliability index is used as reference parameter for the probabilistic assessment.

Keywords: motion-based design, probabilistic approach, reliability, viscous damper, wind-induced vibrations.

1. INTRODUCTION

Cables of cable-stayed bridges are structures prone to vibrate due to wind-induced vibrations. In order to control the dynamic response caused by these vibrations, mechanical passive control systems have been widely used [1, 2]. The objective of this kind of control systems is to install a device which increases the damping of the cable, reducing the amplitude of the dynamic response. Different methods and criteria to design passive control systems have been reported [3]. The first optimum design of passive dampers located near the anchorage was proposed by Kovacs [4] who focused on the effect of a viscous damper installed in a taut cable. The universal curve provided by Pacheco *et al.* [5] represents the modal damping of a taut cable in relation to the damping coefficient of the viscous damper. The use of this curve is limited to the lower natural frequencies of the cable. The analytical expression of this curve was proposed by Krenk [6] who performed a numerical analysis in terms of the solution of a complex eigenvalues problem. Yoneda and Maeda [7] calculated the optimum damping coefficient of a viscous damper and the associated damping ratio of the cable based on the analytical model of a cable.

[1] *Department of Continuum Mechanics and Structural Analysis. Universidad de Sevilla (SPAIN). jnaranjo3@us.es (Corresponding author)*

[2] *Department of Continuum Mechanics and Structures, E.T.S. Ingenieros de Caminos, Canales y Puertos. Universidad Politécnica de Madrid (SPAIN). jf.jimenez@upm.es*

[3] *Department of Continuum Mechanics and Structures, E.T.S. Ingenieros de Caminos, Canales y Puertos. Universidad Politécnica de Madrid (SPAIN). ivan.munoz@upm.es*

[4] *Department of Continuum Mechanics and Structural Analysis. Universidad de Sevilla (SPAIN). andres@us.es*

Although these results are in good agreement and can be employed for the preliminary design of the damper, this study addresses the optimum design of the viscous damper via the solution of a motion-based design problem. This method was first proposed by Connor for the particular case of tall buildings subjected to wind and earthquake excitation [8]. The main advantage of this method is that the size of the installed viscous damper is optimized, as the amplitudes are reduced to meet the standards and not to the maximum allowable reduction. This methodology has been successfully applied by the authors to the optimum design of tuned mass dampers (TMD) for vibration phenomena of footbridges under pedestrian loads [9] and mechanical dampers (viscous, friction and elastomeric) for cables under wind-induced action [10]. The motion-based design methodology allows transforming the problem into a minimization problem subjected to constraints.

The objective of this study is to design a viscous damper based on the motion-based design problem taking into account the uncertainty of the force of the cable. Hence, the design of the viscous damper is not addressed to fulfil the value imposed by the standards but to have a probability of failure below or close to a threshold. Instead of the probability of failure, current guidelines take as reference parameter the reliability index β [11]. The reliability index and the probability of failure are calculated from the probabilistic distribution function of the serviceability limit state function. In order to obtain this probabilistic distribution function, the uncertainty of the axial force is considered and simulated following a probabilistic approach where it is assumed as random variable. Due to the nonlinear behaviour of the cables, a sampling technique is employed to estimate the distribution function. In particular, it is estimated applying the Latin Hypercube simulation method.

The organization of the paper is as follows. First, the damper-cable interaction model is presented. The definition of the viscous damper and the expressions of the wind-induced forces and wind velocities are detailed. Then, the motion-based design optimization problem considering the reliability is explained. Finally, in order to validate the motion-based design method under uncertainty conditions, a viscous damper is designed to reduce the wind-induced vibrations of the longest cable of the Alamillo bridge, in Seville (Figure 1). The result allows installing a damping device whose damping coefficient is less than classical solutions without loss of safety. In addition, the reliability (or the probability of failure) is ensured to be above the threshold. At the end, the main concluding remarks of this paper will be drawn.

a)  b) 

Figure 1. a) Overall view of the Alamillo bridge and b) Viscous damper installed in the longest cable.

2. DAMPER-CABLE INTERACTION MODEL

In order to simulate numerically the behaviour of the damper-cable system, a FE model is built. One of the key aspects when modelling a cable is the bending stiffness. According to the results of [12–14], the bending stiffness of the cable has been considered in this study. The FE model of the cable is built using a 3D beam element (BEAM188) of the software ANSYS [15]. This considered element is a nonlinear two-node beam element with six degrees of freedom at each node. The stress-stiffness option is taken into account herein performing a large strain analysis.

To mitigate the vibration phenomena, a passive damper is implemented in the FE model. In particular, a viscous damper is taken into account for this purpose due to its common use in real practical applications. The viscous dampers are able to dissipate a large amount of energy through a fluid-filled cylinder and a one-directional piston. A linear behaviour of the constitutive law of the viscous damper has been assumed. The viscous damper can be characterized by its damping force $\boldsymbol{F}_v$., which is opposed to the movement of the cable. The definition of $\boldsymbol{F}_v$ depends on the damping coefficient, c [sN/m], and the relative velocity of the damper, $\dot{u}$ [m/s], as it is expressed below:

$$\boldsymbol{F}_v = -c \cdot \dot{\boldsymbol{u}} \tag{1}$$

The element COMBIN14 of the software programme ANSYS was selected to model the viscous damper. This element is defined from the damping coefficient, c.

Finally, the numerical model is finished via the implementation of the wind forces. The expressions of the forces are derived assuming that the cable is a cylinder immersed in a turbulent flow which is characterized by the mean wind velocity, $\mathcal{U}$ [m/s], and the fluctuating velocities $u(t)$ [m/s] and $v(t)$ [m/s] (Figure 2). The former is the longitudinal velocity and the latter is the transverse velocity.

Under the assumptions of quasi-steady model and that the turbulence components are small with respect to $\mathcal{U}$, the forces can be decomposed into a mean and a fluctuating component [16]. Therefore, the drag and lift forces, $F_D(t)$ and $F_L(t)$ [N] respectively, can be derived from a linearized approximation as [17]:

$$F_D(t) = F_D + f_{Du}(t) + f_{Dv}(t) \tag{2}$$

$$F_L(t) = F_L + f_{Lu}(t) + f_{Lv}(t) \tag{3}$$

where F_D is the mean wind drag force, $f_{Du}(t)$ and $f_{Dv}(t)$ are the forces induced by the turbulence component in the drag direction, F_L is the mean lift force and $f_{Lu}(t)$ and $f_{Lv}(t)$ are the forces induced by the turbulence component in the lift direction. The three drag components can be calculated as follows:

$$F_D = 0.5\rho\mathcal{U}DC_D \tag{4}$$

$$f_{Du}(t) = \rho\mathcal{U}u(t)DC_D \tag{5}$$

$$f_{Dv}(t) = 0.5\rho\mathcal{U}v(t)D(C'_D - C_L) \tag{6}$$

Analogously, the three lift components have the expressions:

$$F_L = 0.5\rho\mathcal{U}^2DC_L \tag{7}$$

$$f_{Lu}(t) = \rho\mathcal{U}u(t)DC_L \tag{8}$$

$$f_{Lv}(t) = 0.5\rho\mathcal{U}v(t)D(C_D + C'_L) \tag{9}$$

These six expressions above depend on the density of the air, ρ [kg/m^3], the drag coefficient, C_D, the lift coefficient, C_L and the outer diameter of the cable, D [m]. The parameters C'_D and C'_L are the derivative of C_D and C_L with respect to the angle α at the neighbourhood of β, respectively (Figure 2) [17]. As the section of the cable is assumed to be circular, the variation of these parameters with respect to the angle is nil due to the symmetry. Hence, $C'_L = C'_D = 0$.

Finally, the wind velocities are computed. The numerical simulation of the wind velocity signals can be carried out following several methods. In this study, the wave superposition spectral-based method has been considered for this purpose [18, 19]. This method allows determining numerically the wind velocity as a superposition of trigonometric functions with phase angles set randomly. The power spectral density function of the turbulent wind velocity and the coherence function, which considers the spatial variability of the wind velocity, are used to derive the amplitude of the trigonometric functions. The former is adopted according to the Eurocode 1 [20]. The latter is defined from the relationship proposed by Davenport [21]. The application to simulate the wind action programmed in the package Matlab [22] has been used herein.

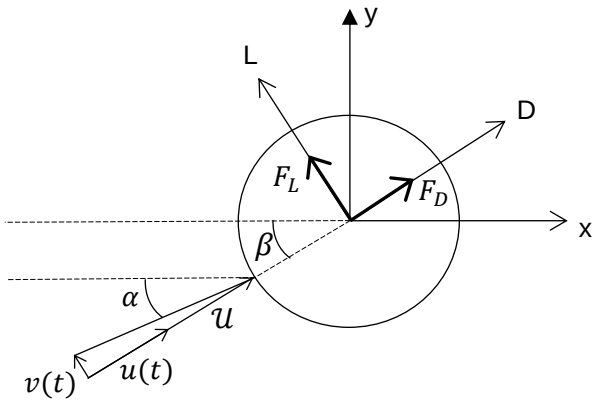

Figure 2. Reference coordinate system, components of the drag and lift forces and wind velocity components.

3. MOTION-BASED DESIGN OF VISCOUS DAMPER UNDER UNCERTAINTY CONDITIONS

Viscous dampers can be designed through the implementation of the motion-based design method [8, 9]. Under this approach, the design requirements are established according to the maximum accepted motions of the structure. Thus, this method allows conducting the design problem as an optimization problem where an objective function is minimized subject to several constraints. The design variable of the minimization problem is the parameter that characterizes the viscous damper, i.e. the damping coefficient, c. The formulation of the minimization problem can be expressed as follows:

$$\text{minimize } f(\boldsymbol{\theta}) \tag{10}$$

$$\text{subject to} \begin{cases} \boldsymbol{\theta}_l < \boldsymbol{\theta} < \boldsymbol{\theta}_u \\ g_k(\boldsymbol{\theta}) \leq g_k^* \quad k = 1, 2, \dots, j \end{cases} \tag{11}$$

where $\boldsymbol{\theta}$ is the vector with the parameters to be found (in this case, only one parameter), $\boldsymbol{\theta}_l$ is the vector with the lower bounds of the parameters, $\boldsymbol{\theta}_u$ is the parameters upper bound vector, $g_k(\boldsymbol{\theta})$ is the k^{th} inequality constraint, g_k^* is the threshold of the k^{th} inequality constraint and j is the number of inequality constraints. In this study, the inequality constraint is defined in terms of the reliability index, β. Probabilistic reliability methods are used to compare the reliability index, β, with its target value, β_t.

$$\beta \geq \beta_t \tag{12}$$

In order to take advantage of the material properties, usually the design is carried out in such a way that the value of the reliability index is minimized to be as close as possible to the target value. The recommended value of the reliability index, β_t, for the serviceability limit state is found in the Eurocode

[23] for a reference period of one year and for fifty years. However, the value for a n-year design can be extrapolated using the following expression:

$$\Phi(\beta_n) = [\Phi(\beta_1)]^n \tag{13}$$

being β_n and β_1 the value of the target reliability index for a n-year and a 1-year design, respectively, and Φ the standard normal cumulative distribution function. In the case of stay-cables, the design is conducted for a life time of 100 years. Therefore, in this study the value of the target reliability index is $\beta_{100} = 0.95$. It is assumed that the expressions of the forces explained above are for a period of 100 years.

The value of β is derived from the limit state function, g, which may be defined under the assumption of g following a log-normal distribution as:

$$g = R/D \tag{14}$$

where R is the resistance of the structure (the maximum allowable response) and D is the demand (the maximum response induced by wind actions). Eq. (14) allows expressing the probability of failure of the limit state as $p_f = \text{Prob}[g < 1]$. The reliability index is calculated for a log-normal distribution as:

$$\beta = \frac{\mu_g}{\sigma_g} = \frac{\text{mean}\left(\ln\frac{R}{D}\right)}{\sqrt{\sigma_{lnR}^2 + \sigma_{lnD}^2}} \tag{15}$$

where σ_{ln} denotes the standard deviation of the log-normal distribution of the variable. The failure probability can be rewritten in terms of β as $p_f = \Phi(-\beta)$. Therefore, for a period of 100 years, the probability of failure must be below the threshold $p_{f_{100}} \leq \Phi(-0.95) = 0.17$. The value of R is adopted following the recommendations of the FHWA guidelines [24] whose compliance criteria of the vibration limit state in terms of the outer diameter of the cable are shown in Table 1. Note that for this particular case, R does not follow a distribution since it is a unique value. Therefore, the standard deviation $\sigma_{lnR}^2 = 0$.

Table 1. User tolerance limits in terms of the outer diameter of the cable, D [24].

Design level	Value [m]
Preferred	$0.5D$
Recommended	$1.0D$
Not to exceed	$2.0D$

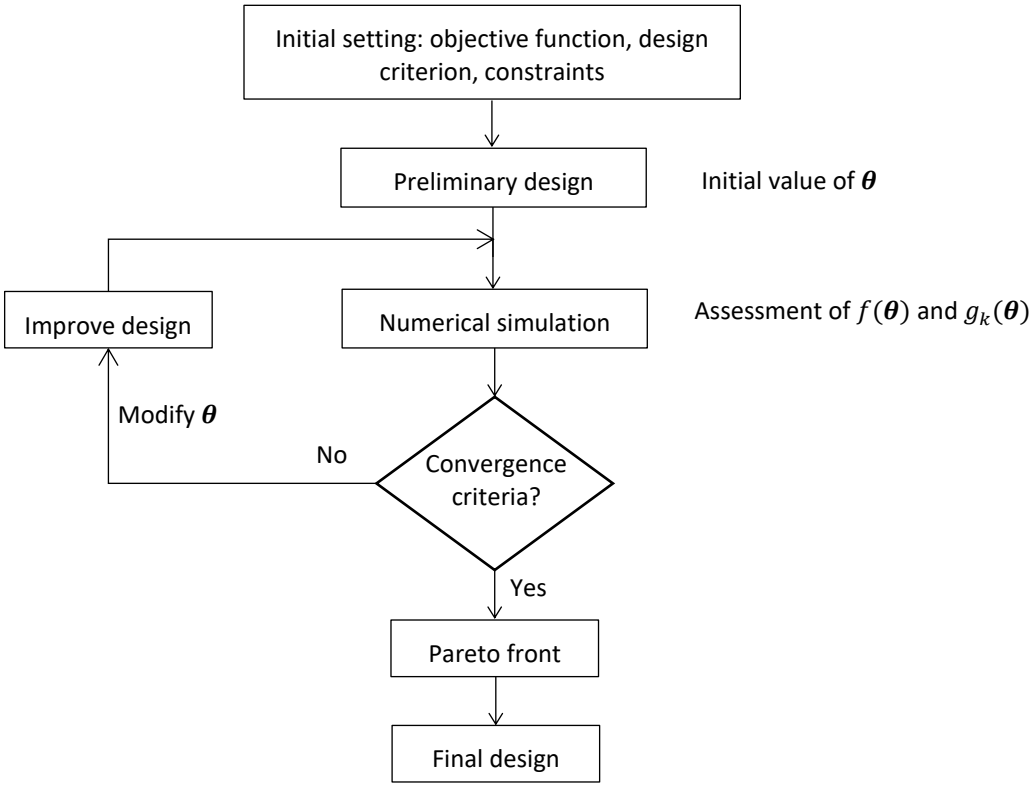

Figure 3. Flowchart of the motion-based design optimization problem.

In this manner, the design of the viscous damper is optimized in order to guarantee the compliance of the requirements based on the motions of the structure with a good level of reliability. The general flowchart of a based-motion design process is shown in Figure 3. First, the objective function, the design parameters and the constraints are established. Subsequently, the preliminary design can be addressed. As result, an initial value of the parameters is obtained. Then, a FE model is built and the response of the system consisting of the structure and the damper is assessed. This evaluation of the dynamic response leads to a first estimation of the objective function. If the convergence criteria of the motion-based design have been reached, the final design is achieved. On the contrary, the parameters must be modified and a new improved design is developed and evaluated. This process is repeated iteratively until the motion-based design requirements are met. The convergence criteria are usually set in terms of the maximum number of iterations and the tolerance of the objective function. As result of the motion-based design procedure, the value of the parameter that minimizes the objective function and meets the constraints is obtained.

The performance of this method is validated in this study through the design of a viscous damper. A real cable of a cable-stayed bridge is considered for the analysis.

4. CASE STUDY

The validation of the motion-based design method is carried out in this study via the design of a viscous damper to mitigate the wind-induced vibrations. As benchmark structure, the Alamillo bridge (Seville)

is considered. This cable-stayed bridge has a length of 200 m and its main characteristic is the absence of back-stays. This absence is addressed through the inclination of the pylon of $32°$ to the vertical. The connection of the pylon to the deck is made with 13 pairs of stays separated by 12 m.

From the dynamics tests performed in 2004 [25], it was reported that the longest stay cables were prone to be affected by vibration phenomena due to rain-wind induced forces and turbulent wind excitation. Hence, the objective of this study is to control the dynamic response of one of these longest stay cables. In particular, the longest stay cable is analysed under turbulent wind forces and rain-wind combination. The following steps are conducted. First, a FE model of the cable is built and the numerical natural frequencies are obtained. The sensitivity of the cable to wind-induced vibrations is analysed based on the natural frequencies. Subsequently, a transient analysis is performed to obtain the dynamic response and the fulfilment of the vibration requirements according to the FHWA guidelines [24] is verified. As this requirement is not met, a viscous damper designed following the motion-based method is implemented.

4.1. FE model and numerical modal analysis

The software package ANSYS [15] is used to build the FE model of the cable. The mechanical and geometrical properties of the analysed cable are given in Table 2. The mesh consisted of 100 equal length elements. The modal analysis was carried out taking into account both the initial stress and stress-stiffening effects. The numerical natural frequencies given in Table 3 were obtained as result of the numerical modal analysis.

From the results shown in Table 3, it can be observed that the cable, as reported in previous research, is prone to suffer vibration phenomena due to both the effect of turbulent wind action (there are natural frequencies below 1 Hz [26]) and the rain-wind induced vibrations (the first six natural frequencies are below 3 Hz [24]). In order to avoid the rain-wind induced problems, the advanced guidelines propose that the damping ratios of the vibration modes whose natural frequencies are below 3 Hz are greater than a reference value. In particular, the FHWA guidelines [24] proposal has been adopted in this study. This approach is based on guaranteeing that the Scruton number for all the vibration modes is above 10:

$$Sc = \frac{m\xi_i}{\rho D^2} > 10 \tag{16}$$

where Sc is the Scruton number, ρ is the density of the air, m is the mass per unit length, ξ_i is the damping ratio of the vibration mode i and D is the outer diameter of the cable. Hence, the damping ratios of the vibration modes must meet the following condition:

$$\xi_i > \frac{10\rho D^2}{m} \tag{17}$$

The mentioned experimental tests show that the experimental damping ratios of the cable did not fulfil this condition. Therefore, a viscous damper should be installed to increase the damping ratios.

Table 2. Geometrical and mechanical properties of the cable.

Parameter of the analyzed cable	Value
Length	292 m
Effective area	0.00838 m^2
Outer diameter	0.20 m
Mass	60 kg/m
Initial axial force	4.13E6 N
Young's modulus	160E9 Pa
Angle with the deck	26°

Table 3. Numerical natural frequencies of the cable.

f_1 [Hz]	f_2 [Hz]	f_3 [Hz]	f_4 [Hz]	f_5 [Hz]	f_6 [Hz]
0.449	0.898	1.348	1.798	2.249	2.699

A transient analysis is conducted to assess the dynamic behaviour of the cable under turbulent wind forces and check the serviceability limit state. If it is not met, the viscous damper must be designed to control the two mentioned problems.

The wind velocity is simulated considering the wave superposition spectral-based method. The duration of the signals and the time step were stablished in $T = 300$ s and $\Delta t = 0.005$ s according to Park *et al.* [27]. The following parameters were adopted for the simulations: basic wind velocity $v_b = 26$ m/s and an environment type III [19]. The mean and the fluctuating wind velocities were obtained at ten different heights of the cable resulting from dividing the cable into equal-length segments. Once the wind velocity was simulated, the forces induced by the wind can be derived (Eq. (2) and Eq. (3)). The density of the air, the drag coefficient and the lift coefficient are assumed to be $\rho = 1.23$ kg/m^3, $C_D = 1.2$ and $C_L = 0.3$, respectively. Figure 4 shows one simulation of the two components of the wind-induced forces at the third height out of ten in which the cable was divided.

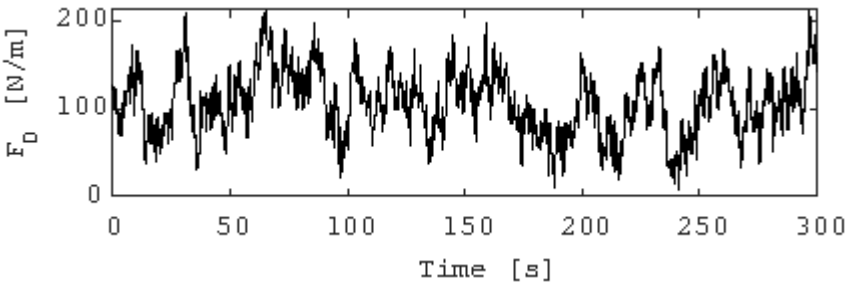

a)

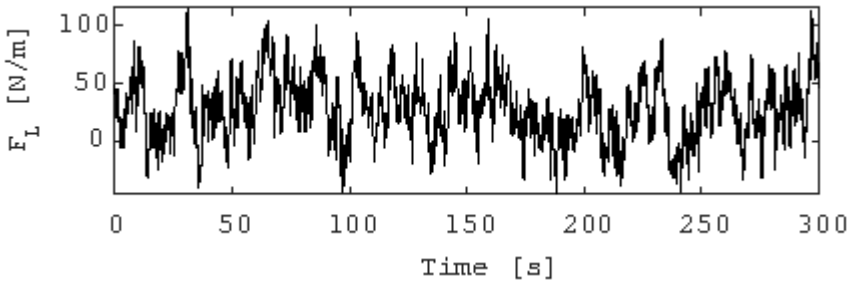

b)

Figure 4. a) Wind-induced drag force at the third height h_3 and **b)** wind-induced lift force at the height h_3.

4.2. Numerical probabilistic simulation of uncertainty and assessment of limit state

The uncertainty associated to the axial force of the cable is simulated through a probabilistic approach. For this purpose, the axial force is considered as a random variable. Following the results of previous research, the axial force of stay cables variate within a range of $\pm 10\%$ [27]. The Latin Hypercube simulation method is used to obtain the distribution function of the reliability index β under wind-induced actions. A key aspect of this simulation method is the number of simulations, N, required. Although empirical relationships between the expected p_f and N have been proposed, such as N equals to one or two orders more than the inverse of p_f, a convergence analysis was performed.

The convergence analysis was performed in two different configurations, without and with viscous damper. For the second configuration, the damping coefficient of the viscous damper has been determined considering the optimum damping coefficient of the Pacheco's universal curve [5]. To obtain its value, the following expression can be used:

$$c_{opt} = 0.10 \cdot \frac{mL\omega_1}{x_c/L} \tag{18}$$

being m the mass per unit length of the cable, L the length of the cable, ω_1 the first natural frequency of the cable and x_c the point where the viscous damper is implemented. According to Caetano [1], this point is recommended to be $x_c = 0.03L$. The result is $c_{opt} = 164000\ \mathrm{sN/m}$. For both configurations, the design criterion of called "Recommended" in Table 1 is selected. It can be observed in Figure 5 that for 100 simulations the value of the parameter β is stabilized. In addition, it can be noticed that the serviceability limit state for the without configuration is not fulfilled as the value of β is negative and, hence, it is lower than the expected value at 100 years: $\beta_{100} = 0.95$. For this reason, it is necessary to install a viscous damper to control the dynamic response of the stay cable. However, it is seen that if the damper is defined from the Pacheco's curve, the serviceability limit state is met but it is not the optimum solution as it is not taken advantage of the properties of the cable ($\beta = 2.76 \gg 0.95$). Therefore, the damping coefficient of the viscous damper should be minimized.

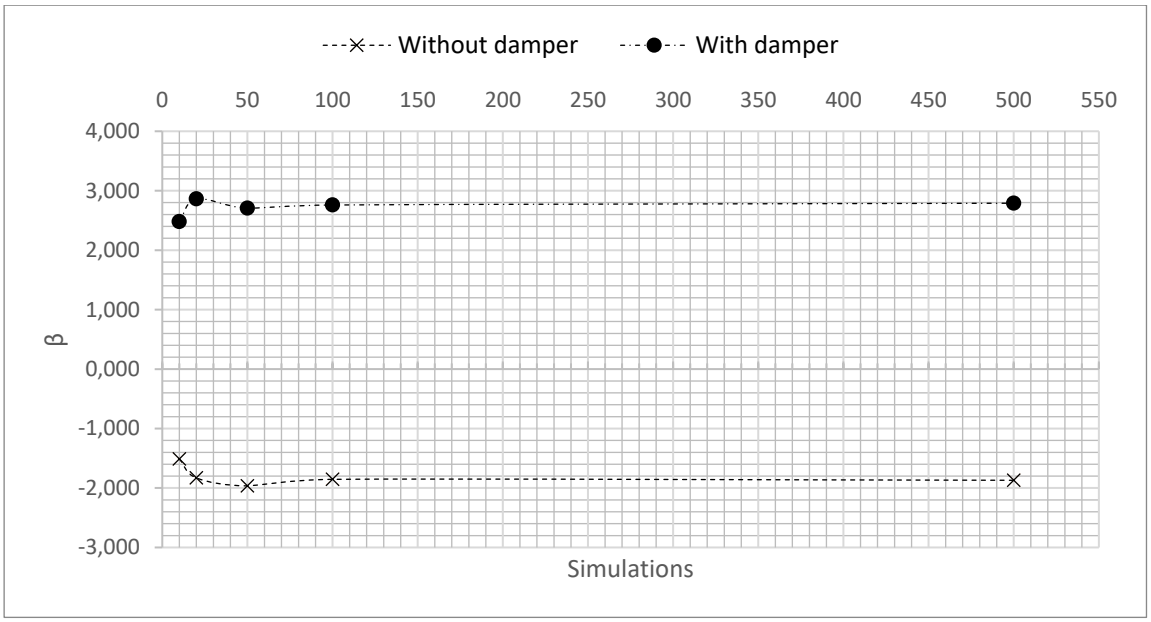

Figure 5. Convergence analysis of the reliability index β for the configuration without damper.

4.3. Motion-based design of the viscous damper under uncertainty conditions

The viscous damper is implemented at the above mentioned point (at a distance of $x_c = 0.03L$ from the anchor). The design is carried out following the proposed motion-based design method under uncertainty conditions. A reduction of the search domain was set in order to improve the efficiency of the algorithm and guarantee that the damping coefficient maintains a physical significance. In the case this study is concerned, there is only one parameter ($\boldsymbol{\theta} = [c]$). The search domain of c guarantees that the maximum dynamic response of the cable and the rain-wind induced vibrations are avoided.

The boundary constraint of the parameter is established in the following manner. The lower bound is set to avoid rain-wind induced vibrations from the limit of the damping ratio of the cable in terms of the Scruton number (Eq. (17)). The analytical expression of the Pacheco's universal curve proposed by Krenk *et al.* [6] allows deriving the damping coefficient from the damping ratio. In this case, the minimum value is $c_{min} = 48500\ \mathrm{sN/m}$. The upper bound is defined as the optimum damping coefficient of the Pacheco's curve.

As optimization algorithm, the gradient-based 'interior-point' as implemented in the software package Matlab [22] is considered. Although this algorithm may fall into a local minimum, its selection to solve the problem is justified from the point that the distribution function is convex and its efficiency to obtain the convergence. The maximum number of iterations is set to 15. The formulation of the motion-based design optimization problem is:

$$\text{find } \boldsymbol{\theta} = c \qquad \text{such that} \qquad \text{minimize } f = c \tag{19}$$

$$\text{subject to} \begin{cases} c_{min} < c < c_{max} \\ \dfrac{\beta_{100}}{\beta} - 1 \leq 0 \end{cases} \tag{20}$$

As result of the minimization problem, the damping coefficient of the viscous damper is obtained. The minimization problem had a duration of $t = 3.57 \cdot 10^5$ s. Table 4 shows the results of the motion-based design problem. It can be observed that the damping coefficient has been minimized guaranteeing that the reliability index is above the expected value at 100 years ($\beta_{100} = 0.95$). For comparison purposes, the reliability indexes obtained from both implementing a viscous damper whose damping coefficient is calculated from the Pacheco's universal curve and without viscous damper are shown as well. Although the value of β could be minimized, it can be noticed the improvement achieved by the motion-based design method with respect to the classical solution. Hence, this method allows meeting the serviceability limit state formulated in terms of the reliability index and obtaining results that better fit to the actual requirements of the structure.

Table 4. Comparison between the Pacheco's optimum solution and the optimized solution (number of simulations = 100).

	Without damper	**Pacheco's optimum**	**Motion-based design**
Damping coefficient, c	-	164000 sN/m	91030 sN/m
Reliability index, β	-1.855	2.760	1.014
Probability of failure, p_f	0.968	0.003	0.155

5. CONCLUSIONS

In this study, a motion-based design under uncertainty conditions has been conducted. In particular, it has been applied to the design of a viscous damper installed in a cable of a cable-stayed bridge in order to reduce the rain-wind induced vibrations. The motion-based design is formulated as a constrained single-objective minimization problem. The objective function to be minimized is the damping coefficient of the viscous damper and the two following constraints are implemented: first, the upper and lower bounds of the damping coefficient in order to maintain a physical significance and improve the efficiency of the algorithm; second, the inequality constraint expressed in terms of the reliability index to guarantee that the reliability index is greater than the expected value at a 100-year design. The uncertainty associated with the variation of the axial force of the cable was simulated numerically following a probabilistic approach. The Latin Hypercube method was used for this purpose.

The performance of this method has been validated for the design of a viscous damper of a real cable-stayed bridge. The results show that the damping coefficient can be minimized from classical solutions without loss of safety since the serviceability limit state is fulfilled. In addition, the reliability has been validated following a probabilistic approach to simulate the variation of the axial force.

ACKNOWLEDGEMENTS

This work was supported by the Ministerio de Economía y Competitividad of Spain and the European Regional Development Fund under project RTI2018-094945-B-C21. The financial support is gratefully acknowledged. J Naranjo Pérez was supported by the research contract from the Universidad de Sevilla Ref: USE-17047-G. The authors acknowledge the financial support provided by the Spanish Ministry of Science, Innovation and Universities through the project SEED-SD (RTI2018-099639-B-I00).

REFERENCES [CALIBRI, 11PT, BOLD, CAPITAL LETTER, LEFT ALIGNMENT]

[1] de Sá Caetano, E. (2007). Cable vibrations in cable-stayed bridges. IABSE.

[2] Ito, M. (1991). Cable-stayed bridges: recent developments and their future. In proceedings of the seminar, Yokohama, Japan, 10-11 December 1991. Elsevier Science Ltd.

[3] Domaneschi, M. & Martinelli, L. (2014). Refined optimal passive control of buffeting-induced wind loading of a suspension bridge. *Wind and Structures, 18, 1, 1–20*.

[4] Kovacs, I. (1982). Zur frage der seilschwingungen und der seildämpfung. *Bautechnik, 59, 10.*

[5] Pacheco, B.M., Fujino, Y. & Sulekh, A. (1993). Estimation curve for modal damping in stay cables with viscous damper. *Journal of Structural Engineering, 119, 6, 1961–1979.*

[6] Krenk, S. (2000). Vibrations of a taut cable with an external damper. *Journal of Applied Mechanics, 67, 4, 772–776.*

[7] Yoneda, M. & Maeda, K. (1989). A study on practical estimation method for structural damping of stay cables with dampers. *Doboku Gakkai Ronbunshu, 410, 455–458.*

[8] Connor, J.J. (2003). Structural Motion Control. Pearson Education, Inc.

[9] Jiménez-Alonso, J.F. & Sáez, A. (2017). Robust optimum design of tuned mass dampers to mitigate pedestrian-induced vibrations using multi-objective genetic algorithms. *Structural Engineering International, 27, 4, 492–501.*

[10] Naranjo-Pérez, J., Jiménez-Manfredi, J., Jiménez-Alonso, J. & Sáez, A. (2018). Motion-based design of passive damping devices to mitigate wind-induced vibrations in stay cables. *Vibration, 1, 2, 269–289.*

[11] Holickỳ, M. (2009). Reliability analysis for structural design. African Sun Media.

[12] Mehrabi, A.B. & Tabatabai, H. (1998). Unified finite difference formulation for free vibration of cables. *Journal of Structural Engineering, 124, 11, 1313–1322*.

[13] Cheng, S., Darivandi, N. & Ghrib, F. (2010). The design of an optimal viscous damper for a bridge stay cable using energy-based approach. *Journal of Sound and Vibration, 329, 22, 4689–4704.*

[14] Hoang, N. & Fujino, Y. (2007). Analytical study on bending effects in a stay cable with a damper. *Journal of Engineering mechanics, 133, 11, 1241–1246.*

[15] Ansys Inc. (2018). Ansys Mechanical 19.0.

[16] Hong, S. (2009). Time domain buffeting analysis of large-span cable-stayed bridge. Porto: Universidade do Porto.

[17] Solari, G. (1994). Chapter: Gust-excited vibrations. In Wind-excited vibrations of structures, Springer, 195-291.

[18] Cremona, C. & Foucriat, J.C. (2002). Comportement au vent des ponts. Presses de l'École Nationale des Ponts et Chaussées.

[19] Jurado Camacho, D. (2017). Simulación estocástica de cargas para análisis dinámico de estructuras en ingeniería civil. Sevilla: Universidad de Sevilla.

[20] EN 1991-1-4. (2005). Eurocode 1: Actions on structures - Part 1-4: General actions - Wind actions.

[21] Davenport, A.G. (1968). The dependence of wind loads on meteorological parameter. *Wind effects on Building and Structures, 19–82.*

[22] MATLAB Inc. (2018). MATLAB R2017b.

[23] EN 1990:2002. (2002). Eurocode 0: Basis of structural design.

[24] Wind-Induced Vibration of Stay Cables. (2007). Publication number: FHWA-HRT-05-083. Federal Highway Administration.

[25] Casas, J.R. & Aparicio, A.C. (2010). Rain–wind-induced cable vibrations in the Alamillo cable-stayed bridge (Sevilla, Spain). Assessment and remedial action. *Structure and Infrastructure Engineering, 6, 5, 549–556.*

[26] Simiu, E. & Scanlan, R.H. (1996). Wind effects on structures: Fundamentals and application to design. John Willey & Sons Inc., 605.

[27] Park, S. & Bosch, H.R. (2014). Mitigation of Wind-Induced Vibration of Stay Cables: Numerical Simulations and Evaluations. United States: Federal Highway Administration. Office of Infrastructure Research and Development.